

# Report on the quality of the LHCb-Muon four-gap MWPC produced at LNF.

## Public Note

Issue:	1
Revision:	0
Reference:	CERN-LHCB-2006-053
Created:	Jan 11, 2006
Last modified:	September 27, 2006
<b>Prepared by:</b>	E. Dané, D. Pinci and A. Sarti



## Abstract

The LNF-LHCb team produced 185 four-gap Multi-Wire Proportional Chambers (MWPC). In this note we report the summary of the results of the panel quality controls and of the measurements performed on the assembled detectors.

## Document Status Sheet

<b>1. Document Title: Report on the quality of the LHCb-Muon four-gap MWPC produced at LNF.</b>			
<b>2. Document Reference Number: CERN-LHCB-2006-053</b>			
<b>3. Issue</b>	<b>4. Revision</b>	<b>5. Date</b>	<b>6. Reason for change</b>
Draft	1	April First, 2006	First version.

## Contents

<b>1</b>	<b>Introduction</b>	<b>3</b>
<b>2</b>	<b>The quality of the wired panels</b>	<b>3</b>
2.1	Wire pitch	3
2.2	Wire mechanical tension	4
<b>3</b>	<b>The quality of the chambers</b>	<b>5</b>
3.1	Gas tightness	6
3.2	Radioactive source test	6
3.3	General remark on gain uniformity: the panel planarity	7
3.4	Criteria for the classification of the chambers	8
3.5	Correction of the gas density effect	8
3.6	Source test results: M3R3 chambers	9
3.7	Source test results: M5R3 chambers	10
3.8	Source test results: M5R4 chambers	12
3.9	Comparison between the different types of chambers	13
3.10	Gain equalization	13

## List of Figures

- 1 Histogram of the wire pitch for all the panels wired in the M3R3, M5R3 and M5R4 chambers production. The solid lines show the  $\pm 50 \mu\text{m}$  requirement, that must be fulfilled at least by the 95% of the wires, while the dashed lines show the  $\pm 100 \mu\text{m}$  requirement, that must be fulfilled by all the wires. The values outside the dashed band come from *fake wire images* (see text and Fig.2). 4

2	Example of pictures of three wires taken by the automated device scanning an M3R3 panel. The picture on the left shows a typical image of three wires used for pitch evaluation. The picture on the right shows an image with a light reflection (on the left), that fakes a wire image and causes the software for the image reconstruction to assign a wrong value to the pitch of the first pair of wires. . . . .	4
3	M3R3 chambers: distribution of the average values of the mechanical tensions of the wires of a panel as a function of the panel number (left) and corresponding histogram (right). . . . .	5
4	M5R3 chambers: distribution of the average values of the mechanical tensions of the wires of a panel as a function of the panel number (left) and corresponding histogram (right). . . . .	5
5	M5R4 chambers: distribution of the average values of the mechanical tensions of the wires of a panel as a function of the panel number (left) and corresponding histogram (right). . . . .	5
6	Leak rate for three different types of chamber: M3R3 (left), M5R3 (centre) and M5R4 (right). . . . .	6
7	Sketch of the chamber built with an exceptionally bent panel (not in scale). . . . .	7
8	Measurement of the bending of the panel 3 (see figure 7) of the chamber in measure are shown on the right. Currents drawn by the two gaps made by using this panel, separately (black triangles) and added (open circles), are shown in the plot on the right. . . . .	7
9	Values of $\Delta G/G_0$ , obtained with the old (left) and new (right) gas mixture, are shown as a function of $\Delta T/T_0 - \Delta P/P_0$ . . . . .	9
10	Values of $\bar{I}_g^c$ for the four gaps of the M3R3 chambers. Vertical bars show $\Delta I_g^c$ found in all gaps. . . . .	10
11	Values of $\bar{I}_b^c$ for the two double-gaps of the M3R3 chambers. Vertical bars indicate the maximum spread of current. . . . .	10
12	Values of $\bar{I}_g^c$ for the four gaps of the M5R3 chambers. Vertical bars show $\Delta I_g^c$ found in all gaps. . . . .	11
13	Values of $\bar{I}_b^c$ for the two double-gaps of the M5R3 chambers. Vertical bars indicate the maximum spread of current. . . . .	11
14	Values of $\bar{I}_g^c$ for the four gaps of the M5R4 chambers. Vertical bars show $\Delta I_g^c$ found in all gaps. . . . .	12
15	Values of $\bar{I}_b^c$ for the two double-gaps of the M5R4 chambers. Vertical bars indicate the maximum spread of current. . . . .	12
16	$\bar{I}_g^c$ values for all the gaps of the 184 chambers tested. . . . .	13
17	Values of $\bar{I}_b^c$ for the double-gaps of all the 184 four-gap chambers tested. Vertical bars indicate the maximum current spread found. . . . .	14
18	Total gain spreads for the double-gaps of all the 184 four-gap chambers tested rescaled in order to equalize the values of $\bar{I}_b^c$ . . . . .	14

## List of Tables

1	Summary of the setup (gas mixture and reference chamber) used for the gain measurements. . . . .	9
2	Average values and rms of $\bar{I}_g^c$ and mean of $\Delta I_g^c$ for the four gaps of the M3R3 chambers after the correction for the effects of T and P variations. . . . .	10
3	Average values and rms of $\bar{I}_g^c$ and mean of $\Delta I_g^c$ for the four gaps of the M5R3 chambers after the correction for the effects of T and P variations by means of the reference chamber data. . . . .	11
4	Average values and rms of $\bar{I}_g^c$ and mean of $\Delta I_g^c$ for the four gaps and the double-gaps of the M5R4 chambers after the correction for the effects of T and P variations by means of the reference chamber data. . . . .	12

## 1 Introduction

The LHCb experiment is dedicated to study the decays of beauty hadrons at LHC. The Level-0 trigger of the experiment calls for fast measurement of the muon transverse momentum and a high capability of bunch-crossing identification. The muon detector must therefore have a high detection efficiency and a good spatial and time resolution. The LHCb muon detector (1) is composed of five tracking stations (M1–M5) which comprise 1368 Multi Wire Proportional Chambers (MWPC) now under construction in different sites: CERN (CH), LNF-Frascati (ITA), Ferrara (ITA), Firenze (ITA) and PNPI-San Petersburg (RU).

The 5 mm high gas gap, is filled with an Ar/CO<sub>2</sub>/CF<sub>4</sub> (40/55/5) gas mixture. The anode plane is composed of 30 μm diameter gold-plated tungsten wires with a pitch of 2 mm. While chambers in station M1 will be composed of two single-gaps the ones of stations M2–M5 are composed of two double-gaps (four-gap chambers in the following) in which the corresponding pads are ganged in pairs. The front-end electronics performs a further logical OR between the two signals of the single (double) gaps.

At LNF 185 four-gap MWPC ((2) and (3)) were assembled in almost one and a half year. Three different types of chambers were produced:

- 58 M3R3 chambers which have 664 wires per gap that are 295 mm long;
- 59 M5R3 and 68 M5R4 chambers which have 760 wires per gap that are 325 mm long.

The assembly procedure foresees a set of controls to check the quality of the wired panels and of the assembled chambers. The results of those tests are summarized in this note.

## 2 The quality of the wired panels

After the wire winding all the panels were tested. As described in details in (2), in a completely automated way, both pitch and the mechanical tension of all the wires were measured and the results were recorded in a database (4).

### 2.1 Wire pitch

The wire pitches were measured with a device based on two digital cameras as explained in (2). The requirement on the values of the wire pitch (WP) is:

$$\begin{aligned} \text{WP} &= 2.00 \pm 0.05 \text{ mm [for at least the 95\% of the wires]} \\ \text{WP} &= 2.00 \pm 0.10 \text{ mm [for the 100\% of the wires]} \end{aligned}$$

The results of all the measurements performed are shown in figure 1. Nearly all the data points are inside the allowed region. The pictures of the wires with pitches outside from the dashed lines region have been optically checked one by one. In all cases (about 600 wires in 680 panels) they were found to come from a *fake wire image* as the one shown in figure 2. In that picture the effect of a light reflection on the black surface underlying the wires can be clearly seen: the software for the image analysis reconstructs four wires instead of three, and assign a wrong value to the first pitch measured. In fact, only 4 wires (corresponding to 0.001% of the whole production) needed to be replaced because a wrong pitch was found. After those replacements all other pitches measured (more than 500 k) were found to be within the above requirements.

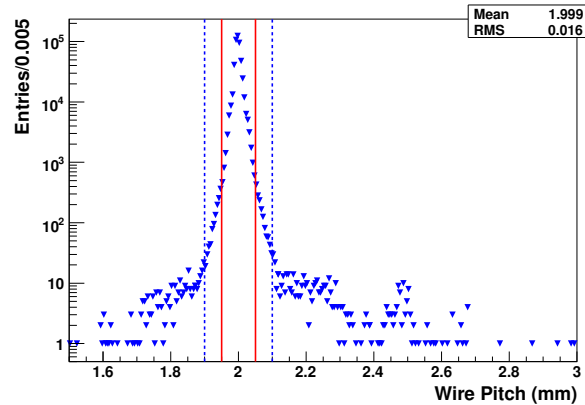


**Figure 1** Histogram of the wire pitch for all the panels wired in the M3R3, M5R3 and M5R4 chambers production. The solid lines show the  $\pm 50 \mu\text{m}$  requirement, that must be fulfilled at least by the 95% of the wires, while the dashed lines show the  $\pm 100 \mu\text{m}$  requirement, that must be fulfilled by all the wires. The values outside the dashed band come from *fake wire images* (see text and Fig.2).

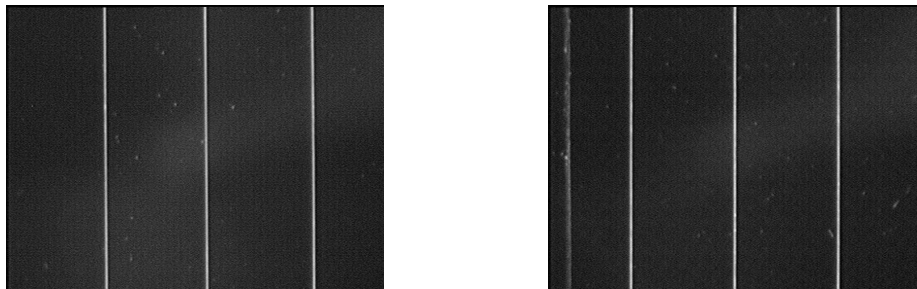


**Figure 2** Example of pictures of three wires taken by the automated device scanning an M3R3 panel. The picture on the left shows a typical image of three wires used for pitch evaluation. The picture on the right shows an image with a light reflection (on the left), that fakes a wire image and causes the software for the image reconstruction to assign a wrong value to the pitch of the first pair of wires.

## 2.2 Wire mechanical tension

The mechanical tension of the wires of the chambers produced was measured by means of a machine described in (2), in (5) and in (6). In order to ensure electrostatic and mechanical stability the wire mechanical tension value is required to be in the range 0.5 N - 0.9 N. In the figures 3, 4 and 5 the average values of the mechanical tensions of all the wires of a panel are shown as a function of the panel number along with the corresponding histograms. Two peaks are clearly visible in the histograms of the M5R3 and M5R4 chambers: this reflects the fact that the voltage of the torque motor, which controls the tensioning of the wire during the winding, was changed during the production. In particular the production of the M3R3 chambers was the first one and the wiring procedure needed a fine tuning and a long people training. More than  $5 \times 10^5$  wire tensions were measured. A total of 600 wires (corresponding to 0.11% of the whole production) has been replaced because of their the mechanical tension was found to be below 0.50 N. After those replacements all the mechanical tensions measured were well inside the above requirements.

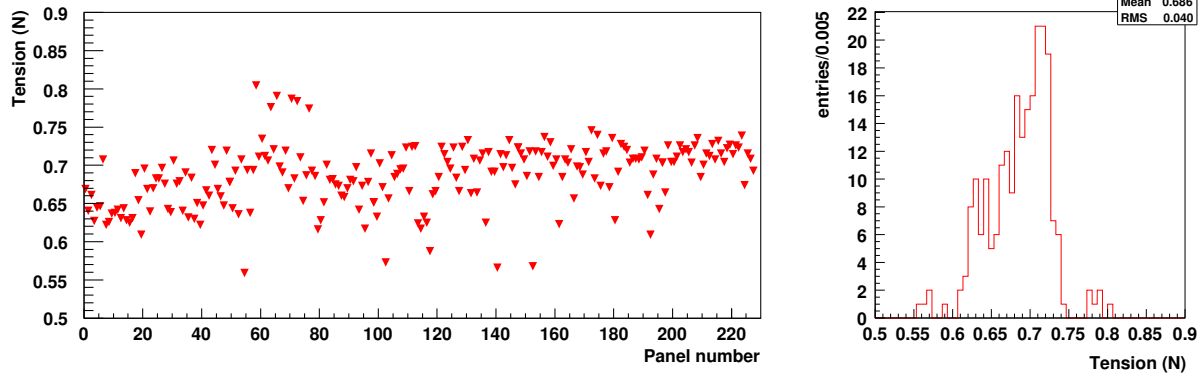


**Figure 3** M3R3 chambers: distribution of the average values of the mechanical tensions of the wires of a panel as a function of the panel number (left) and corresponding histogram (right).

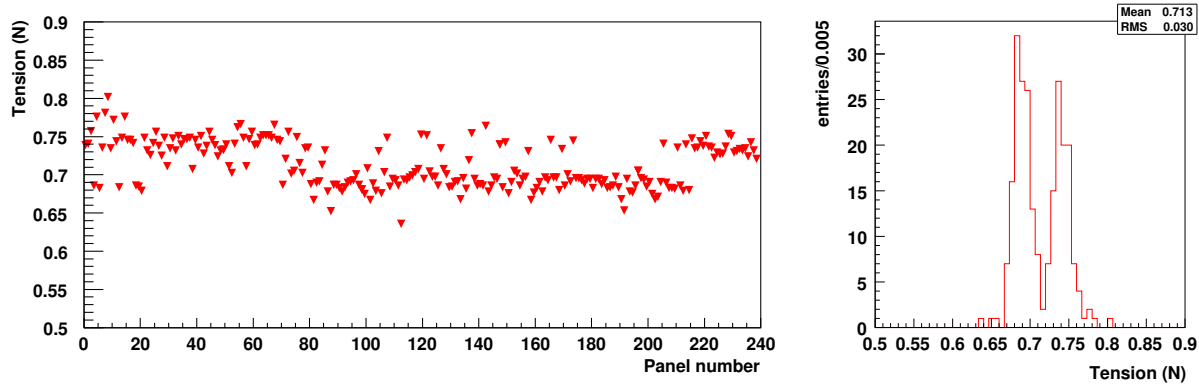


**Figure 4** M5R3 chambers: distribution of the average values of the mechanical tensions of the wires of a panel as a function of the panel number (left) and corresponding histogram (right).

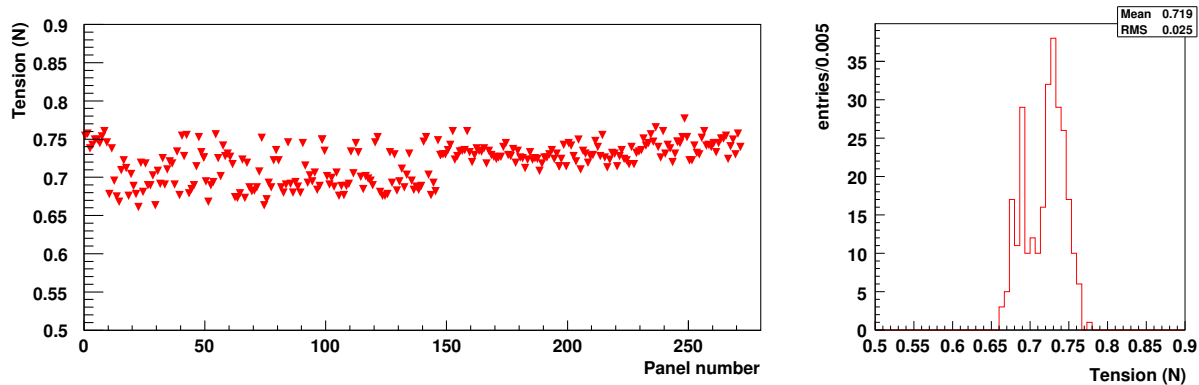


**Figure 5** M5R4 chambers: distribution of the average values of the mechanical tensions of the wires of a panel as a function of the panel number (left) and corresponding histogram (right).

### 3 The quality of the chambers

Each chamber was tested, shortly after its assembly, to check the gas tightness quality. After a suitable high voltage conditioning the gas gain uniformity of the four gaps of each chamber was measured by means of a radioactive source. The results, corrected for the effects of the variations of the gas temperature and pressure are shown in the following sections.

## 3.1 Gas tightness

The chambers gas leakage was measured by monitoring the decrease in time of an overpressure of 5 mbar. The method, described in more details in (2) and (5), has a sensitivity of about 0.01 mbar/hour well below the maximum gas leakage accepted (2 mbar/hour). The results of the measurements are

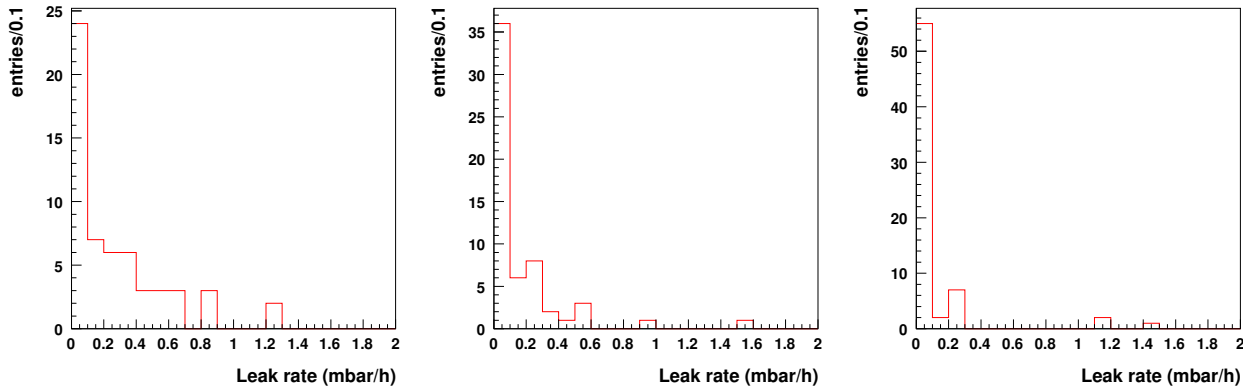


**Figure 6** Leak rate for three different types of chamber: M3R3 (left), M5R3 (centre) and M5R4 (right).

shown in figure 6:

- 84 chambers have a rate of leakage lower than the above sensitivity;
- 96 chambers have a rate of leakage between 0.02 and 1.6 mbar/hour;
- 4 chambers showed gas leakages as high as it was difficult to keep an overpressure inside them;
- in one case (chamber 3 of M3R3 type) the gas leakage was as high as it was impossible to perform a safe high voltage conditioning.

From figure 6, by comparing the population of the first bin in the different histograms, it can be seen that the amount of chambers having a small gas leakage rate increased during the production (M5R3 production has followed the M3R3 one and has been followed by the M5R4 one).

## 3.2 Radioactive source test

All the produced chambers (apart from chamber 3 of type M3R3, see section 3.1) after a suitable high voltage conditioning were tested by means of a radioactive source as described in details in (2) and (5). The current drawn by each gap was recorded while the source was moved in 144 different positions on the chamber surface. This test provides two main informations on the chamber quality:

1. the average  $\bar{I}_g^c$  of the 144 values ( $I_g^c(x,y)$ ) of the current drawn by the gap  $g$  of chamber  $c$  (while the source was in the position  $(x,y)$ ) recorded during the source scan gives information on the absolute gas gain of the gap;
2. the spread of the values of  $I_g^c(x,y)$  describes the uniformity of the gas gain in a gap. In particular we will report the values of  $\Delta I_g^c$  defined as the difference between the maximum and minimum current measured in the gap  $g$  of chamber  $c$ .



Both the mean value and the uniformity of the gas gain are directly related to geometrical parameters as the gap height, the wire pitch and the position of the anode plane inside the gas gap (7). Thus, the knowledge of the behaviour of the gas gain inside the gaps was an useful tool to have a fast feedback on the quality of the production procedure. It is also important to outline that two different gas mixtures were used for the source test. A first part of chambers was tested with an Ar/CO<sub>2</sub>/CF<sub>4</sub> 40/40/20 (referred as *old* in the following). Then, we decided to use the mixture which will be used in the experiment: Ar/CO<sub>2</sub>/CF<sub>4</sub> 40/55/5 (referred as *new* in the following).

### 3.3 General remark on gain uniformity: the panel planarity

The measurements of the wire pitch and mechanical tension (sections 2.1 and 2.2) showed that the quality of the wiring fulfills all the requirements. Thus, in general, the cause of possible gain disuniformities and variations should be searched elsewhere. A very critical parameter is the planarity of the panels used to build the gas gaps. Variations of the planarity (i.e. small bending of panels) give rise to variations of the gap height. From Monte Carlo studies of the chamber performance (7) a gain variation of about 25% (50%) was expected for gap height variation of 90 (180)  $\mu\text{m}$  from the nominal one (5mm). In order to check the effect of the planarity of the cathode panels we measured the gas gain in two gaps made by using an exceptionally bent panel, as shown in figure 7. In figure 8 the

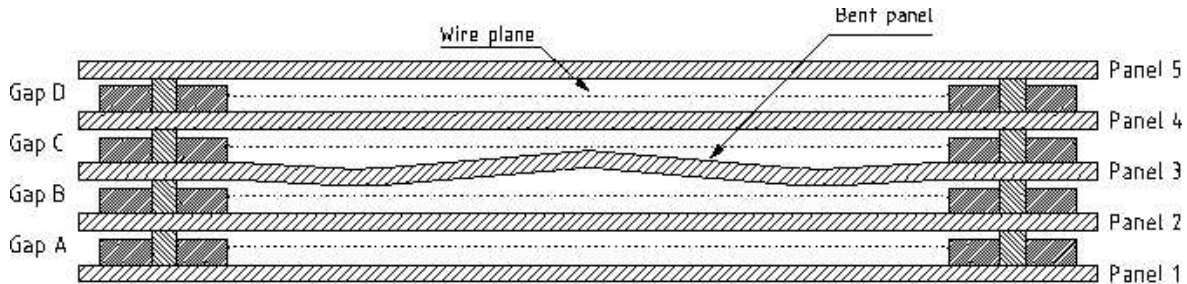


**Figure 7** Sketch of the chamber built with an exceptionally bent panel (not in scale).

measurements of the bending of panel 3 (which reflect on deviations of the height of the gap B and C) are shown on the left while the plot of the currents drawn by the gap C (alone) and by the gaps C and B (added up) is shown on the right. In the centre the panel showed a bending of about 200  $\mu\text{m}$  on

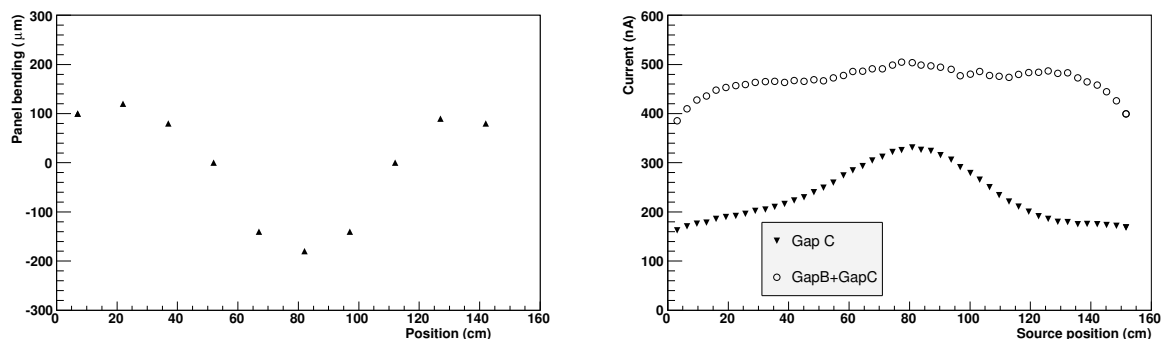


**Figure 8** Measurement of the bending of the panel 3 (see figure 7) of the chamber in measure are shown on the right. Currents drawn by the two gaps made by using this panel, separately (black triangles) and added (open circles), are shown in the plot on the right.

the side that was faced to the gap C (that means a decrease of the gap C height of 200  $\mu\text{m}$ ) and at the ends a bending up to 100  $\mu\text{m}$  on the side faced to the gap B (with a corresponding increase of gap C

height of 100  $\mu\text{m}$ ). At a distance of 50 cm and 110 cm from the panel border, where no bending was measured, the same values of current were measured (about 230 nA).

The variations of the currents measured are in good agreement with the expected values: in the centre of the gap C there was an increment of the gain of about 50% while in both ends of the chamber a decrease of gain of about 22% was found. Moreover, the fact that the sum of the current of gap B and gap C was almost constant (figure 8) was a clear indication that the gain dis-uniformity was due to the bending of the panel between them. The drop of the current on both ends of the chamber was due to a "border" effect: when the source was close to the chamber edges, a part of the photons escaped the sensitive area decreasing the observed current.

### 3.4 Criteria for the classification of the chambers

As already described in (2) and (5) the chambers are classified on the basis of the results of the source scan. In particular, because the front-end electronics sees the four gaps as two double-gaps, the classification criteria are based on the double-gap data. Each double-gap is classified, accordingly to the uniformity of the values of the current  $I_c^d(x,y)$ , in one of the following two categories:

$$\text{Category I: } 1/1.5 \leq I_c^d(x,y)/I_0 \leq 1.5 \quad \forall x \text{ and } y \quad (1)$$

$$\text{Category II: } 1/1.7 \leq I_c^d(x,y)/I_0 \leq 1.7 \quad \forall x \text{ and } y \quad (2)$$

where  $I_0$  is the current drawn by a double-gap at the nominal gain  $G_0$ . A chamber with no more than one double-gap exceeding the requirements of category I and within the limits of category II is considered *good*. A chamber having both double-gaps belonging to the category II (and both outside from category I) is considered *spare* and a chamber having at least one double-gap outside from category II is a *rejected* chamber.

In this paper we will show both the results of the current measurements for the single-gaps for systematic effect studies, and the results of the double-gaps for chamber classification. In particular, in the plots regarding the double-gaps horizontal lines representing the above limits will be shown.

### 3.5 Correction of the gas density effect

The absolute gain value in a MWPC is a function of the gas density which depends on the gas temperature  $T$  and pressure  $P$  (8):

$$\frac{\Delta G}{G_0} = \alpha \left( \frac{\Delta P}{P_0} - \frac{\Delta T}{T_0} \right) \quad (3)$$

In order to compare gain measurements taken in different environmental conditions, the knowledge of  $T$ ,  $P$  and  $\alpha$  is needed. To evaluate the value of  $\alpha$  we studied the behaviour of the average current of a chamber as a function of  $T$  and  $P$  that are monitored with an accuracy of 0.1 K and 1 mbar respectively. In figure 9 the value of  $\Delta G/G_0$  with *old* (*new*) gas mixture is plotted in the left (right) plot as a function of  $\Delta T/T_0 - \Delta P/P_0$ .  $\Delta G$  is defined as  $G - G_0$  and  $G_0$  is the gain of the chamber in a *reference* measurement with  $T = T_0$  and  $P = P_0$ . The values of  $T_0$  and  $P_0$  for the *old* (*new*) gas mixture *reference* measurements were  $P_0=990$  mbar (998 mbar) and  $T_0=300.5$  K (295.7 K). From a linear fit we extracted the value of  $\alpha$ :  $6.32 \pm 0.22$  for the *old* gas mixture and  $5.34 \pm 0.39$  for the *new* one. The latter is in good agreement with the one found in literature (8). Each  $\Delta G/G_0$  value was obtained from the average of the values  $I(x,y)/I_0(x,y) - 1$  measured in 144 different chamber points. The errors on  $\Delta G/G_0$  shown in both plots have been estimated by using the RMS of the  $I(x,y)/I_0(x,y) - 1$  distributions. The large errors shown for some measurements can be explained by the temperature variations during the source scan (which lasts about one hour). Once the value of  $\alpha$  was known it was possible to correct the effects of  $T$  and  $P$  variations, by multiplying the measured currents by  $f$ :

$$f = \frac{1}{\alpha \left( \frac{\Delta P}{P_0} - \frac{\Delta T}{T_0} \right) + 1}$$

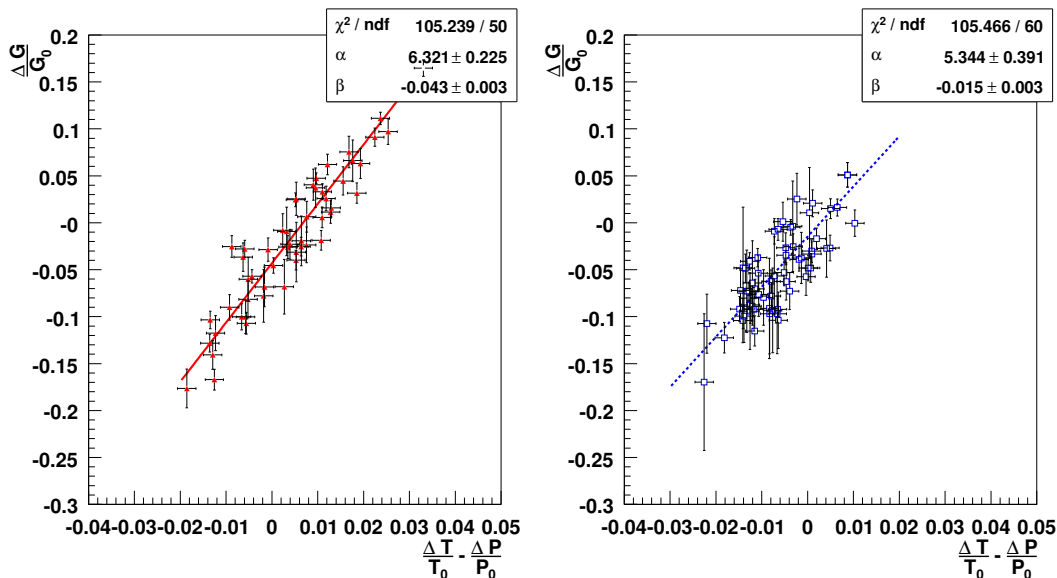


**Figure 9** Values of  $\Delta G/G_0$ , obtained with the old (left) and new (right) gas mixture, are shown as a function of  $\Delta T/T_0 - \Delta P/P_0$ .

The monitoring of the temperature of the gas flushed into the chamber was difficult. After the first 69 chambers had been tested we decided to place a *reference* one-gap chamber on the table below the chamber under test gas flushed in series with it to compensate the effects of T and P. In table 1 the test conditions for all the chambers are summarized.

**Table 1** Summary of the setup (gas mixture and reference chamber) used for the gain measurements.

Chamber type	Old mixture	Old mixt. and ref. chamber	New mixt. and ref. chamber
M3R3	1,2,4-58	-	-
M5R3	1-11	12-48	49-59
M5R4	-	1-13	14-68
Tot	68	50	66

In the following we present the results of the source tests for the three different types of chambers (M3R3, M5R3 and M5R4) separately. All the values of the current measured have been corrected for the T and P effects: by using the correction factor  $f$  or the information given by the *reference* chamber when available.

### 3.6 Source test results: M3R3 chambers

In figure 10 the values of  $\bar{I}_g^c$  for the four gaps of the M3R3 chambers are plotted. Vertical bars indicate the maximum spread ( $\Delta I_g^c$ ) of  $I_g^c(x,y)$  found in each gap. In figure 11 the same is shown for the double-gaps. The main results are summarized in table 2. The mean values of the gain of the four gaps in table 2 are consistent with the average values reported in the last row. The  $\Delta I_g^c$  values are quite consistent. This indicates that the four gaps have similar absolute gain and gain uniformity. The ratios between the rms and mean values of  $\bar{I}_g^c$  is in the range 13%–20%. Only the chamber number 58 has both the double-gaps outside from Category I. No chamber was found with both double-gaps outside from limits of Category II. Hence, all the M3R3 chambers tested, but the number 58 classified *spare*, are considered *good*.

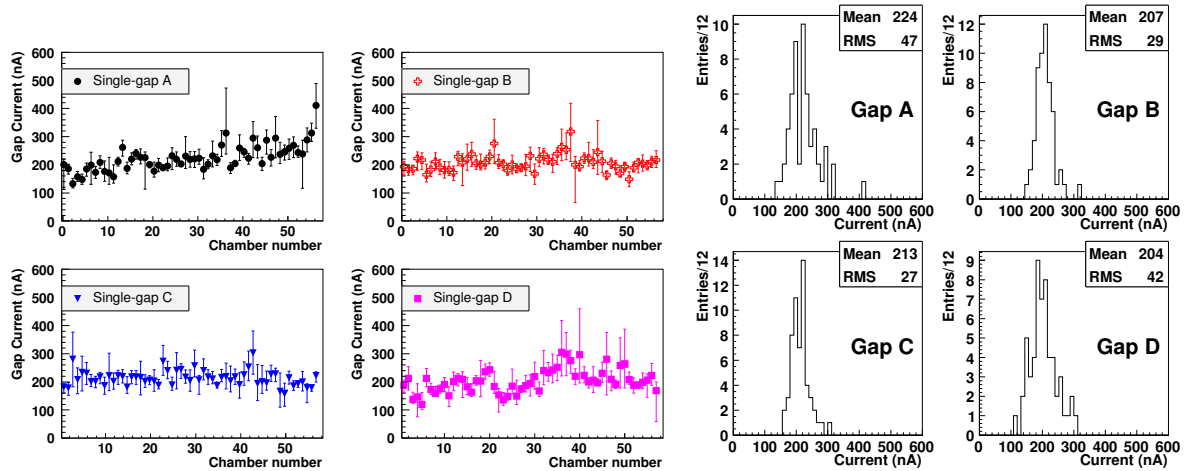


Figure 10 Values of  $\bar{I}_g^c$  for the four gaps of the M3R3 chambers. Vertical bars show  $\Delta I_g^c$  found in all gaps.

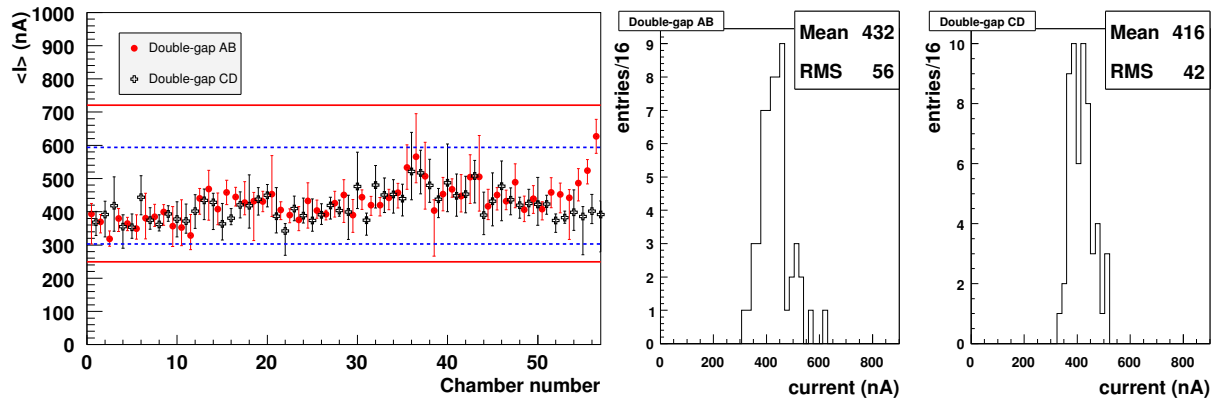


Figure 11 Values of  $\bar{I}_b^c$  for the two double-gaps of the M3R3 chambers. Vertical bars indicate the maximum spread of current.

Table 2 Average values and rms of  $\bar{I}_g^c$  and mean of  $\Delta I_g^c$  for the four gaps of the M3R3 chambers after the correction for the effects of T and P variations.

	mean	rms	rms/ $\sqrt{57}$	$\Delta I_g^c$
Gap A	224	47	5.9	66
Gap B	207	29	3.5	65
Gap C	213	27	3.5	71
Gap D	204	42	5.1	80
Mean	212			71
Double-Gap AB	432	56	7.0	95
Double-Gap CD	416	42	5.1	105

### 3.7 Source test results: M5R3 chambers

In figure 12 the mean  $\bar{I}_g^c$  values for each M5R3 gap are reported. In figure 13 the same is shown for the double-gaps. In figure 12 an increasing trend in the average values of the gain of gap D can be seen: the last chambers built have a higher gain with respect to the first ones. This effect was probably due to a decrease of the gap D size during the production phase that was in part related to a change we made in the assembly procedure, needed to increase the gain in the gap D which was lower than in the others gap (up to chamber 20), and in part related to the poor planarity of the panels used

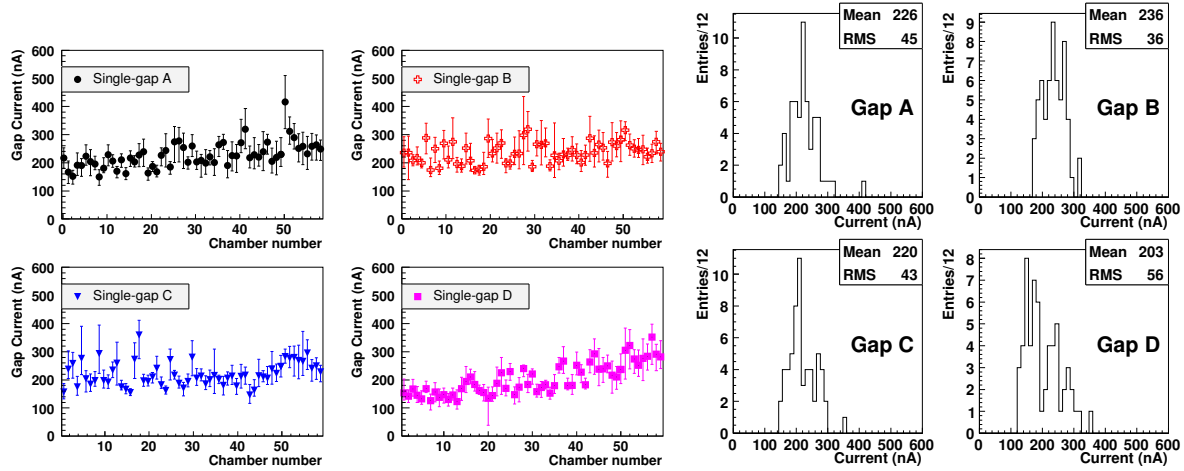


Figure 12 Values of  $I_g^c$  for the four gaps of the M5R3 chambers. Vertical bars show  $\Delta I_g^c$  found in all gaps.

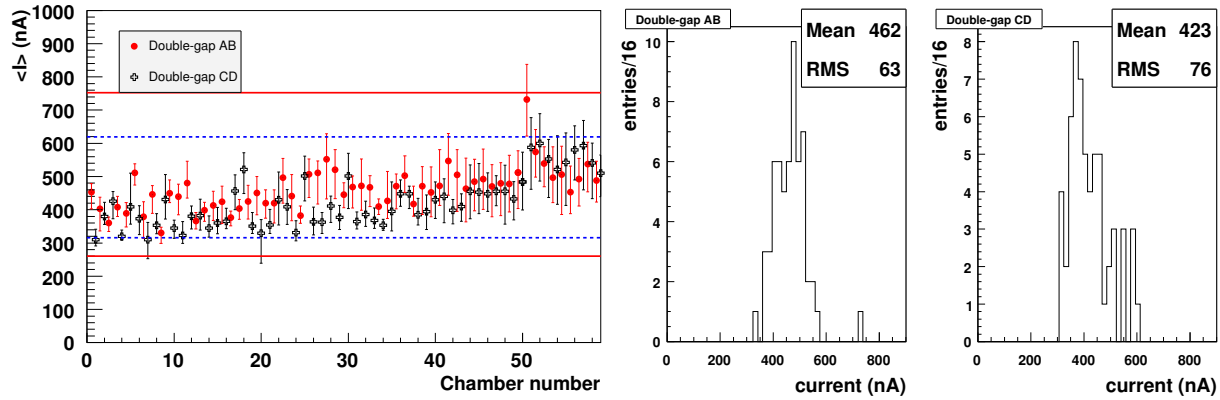


Figure 13 Values of  $I_b^c$  for the two double-gaps of the M5R3 chambers. Vertical bars indicate the maximum spread of current.

to assemble the last chambers. It is important to underline that the chambers 49–59, were assembled after the whole production of the M5R4 ones. This can explain why the average gain of the last 11 chambers resulted to be slightly different from the one of the other M5R3. The summary of the results of the gain measurement is shown in table 3.

The ratio between the averages of  $I_g^c$  and the rms is in the range 15-20 % for gaps A, B and C and 27 %

Table 3 Average values and rms of  $I_g^c$  and mean of  $\Delta I_g^c$  for the four gaps of the M5R3 chambers after the correction for the effects of T and P variations by means of the reference chamber data.

	mean	rms	rms/ $\sqrt{59}$	$\Delta I_g^c$
Gap A	226	45	7.7	91
Gap B	236	36	6.7	96
Gap C	220	43	7.2	80
Gap D	203	56	8.8	84
Mean	221			88
Double-Gap AB	462	63	9.2	130
Double-Gap CD	423	76	11.2	120

for gap D. Three *rejected* (7, 20 and 50), one *spare* (51) and 55 *good* chambers were found (figure 13).

### 3.8 Source test results: M5R4 chambers

The values of  $\bar{I}_g^c$  and  $\Delta I_g^c$  for the M5R4 chambers tested are reported in figure 14 for the four gaps and in figure 15 for the double-gaps. The summary of the results of the gain measurement are reported in

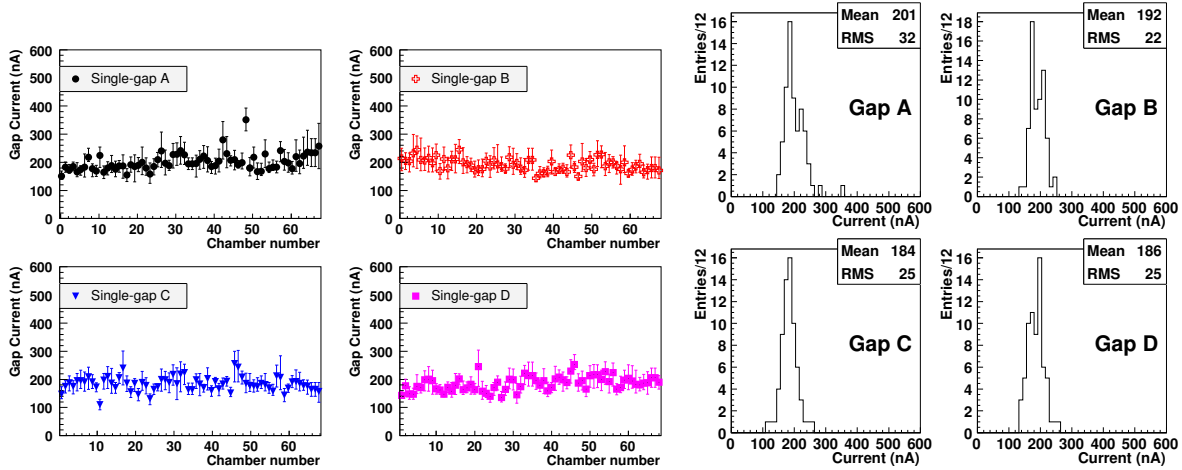


**Figure 14** Values of  $\bar{I}_g^c$  for the four gaps of the M5R4 chambers. Vertical bars show  $\Delta I_g^c$  found in all gaps.

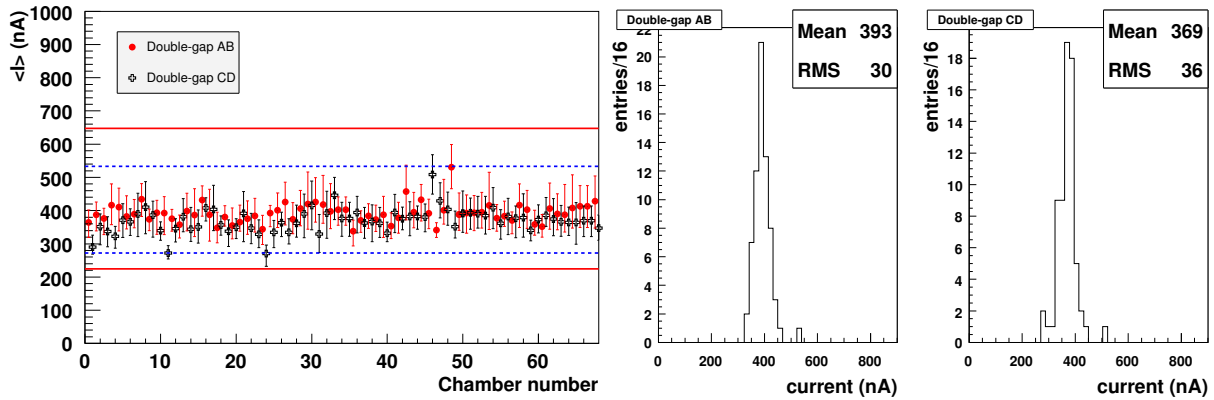


**Figure 15** Values of  $\bar{I}_b^c$  for the two double-gaps of the M5R4 chambers. Vertical bars indicate the maximum spread of current.

table 4. The four gaps of the M5R4 chambers have consistent absolute gain values and gain unifor-

**Table 4** Average values and rms of  $\bar{I}_g^c$  and mean of  $\Delta I_g^c$  for the four gaps and the double-gaps of the M5R4 chambers after the correction for the effects of T and P variations by means of the reference chamber data.

	mean	rms	rms/ $\sqrt{68}$	$\Delta I_g^c$
Gap A	201	32	5.3	78
Gap B	192	22	4.2	75
Gap C	184	25	4.4	63
Gap D	186	25	4.4	67
Total	190			71
Double-Gap AB	393	30	4.0	120
Double-Gap CD	369	36	4.8	106

mities. The ratio rms/mean ranges from 11% to 16% for all the four gaps. All the 68 M5R4 chambers produced are *good*.

### 3.9 Comparison between the different types of chambers

In figure 16 the values of  $\bar{I}_g^c$  for all the gaps of the 184 chambers tested are shown. The average gap current is 216 nA with a total rms of 42 nA (the ratio being equal to 19%). The mean value of  $\Delta I_g^c$  is 76.7 nA. The M5R3 chambers have a quite high gain in all the four gaps, while the mean values of the gain of the gaps for the M3R3 and M5R4 chambers are similar. In particular the gaps B of M5R3 chambers are in average the ones with the highest current (236 nA) while the gaps C of M5R4 chambers are the ones with the lowest one (184 nA). The gain uniformity within the gap ( $\Delta I_g^c$ ) is quite constant over the whole production ranging from the 30% of the mean  $\bar{I}_g^c$  for gaps A of M3R3 chambers to 40% for the gaps D of the M3R3 chambers. Also the gain uniformity within the double-gap ( $\Delta I_b^c$ ) is quite constant over the whole production (23% of the mean  $\bar{I}_b^c$  for double-gaps AB of M3R3 chambers to 28% for the double-gaps AB of the M5R4 chambers). The fact that the ratio between the total spread and the average gain of the single-gaps is higher than the same value for the double-gaps is a clear sign that a large part of the gain dis-uniformity is due to the bad planarity of some panels.

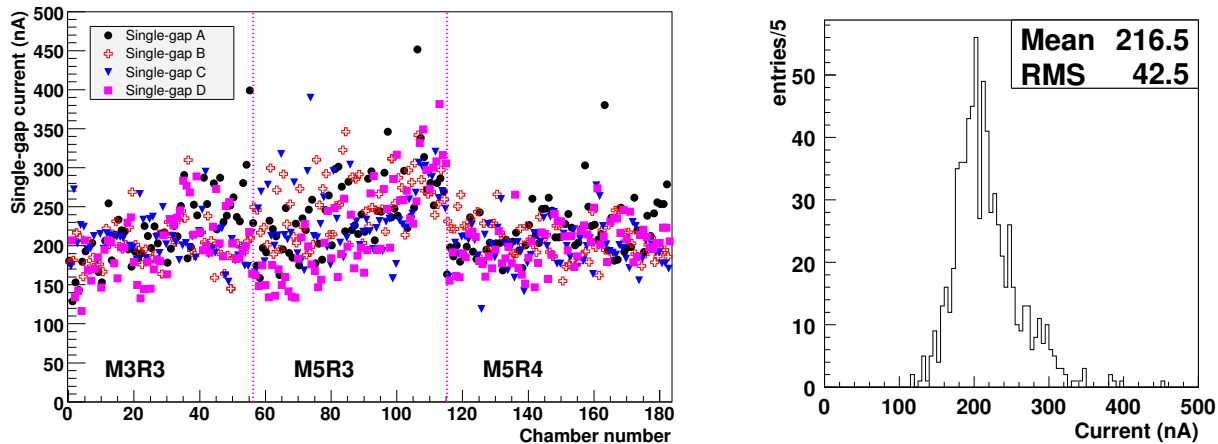
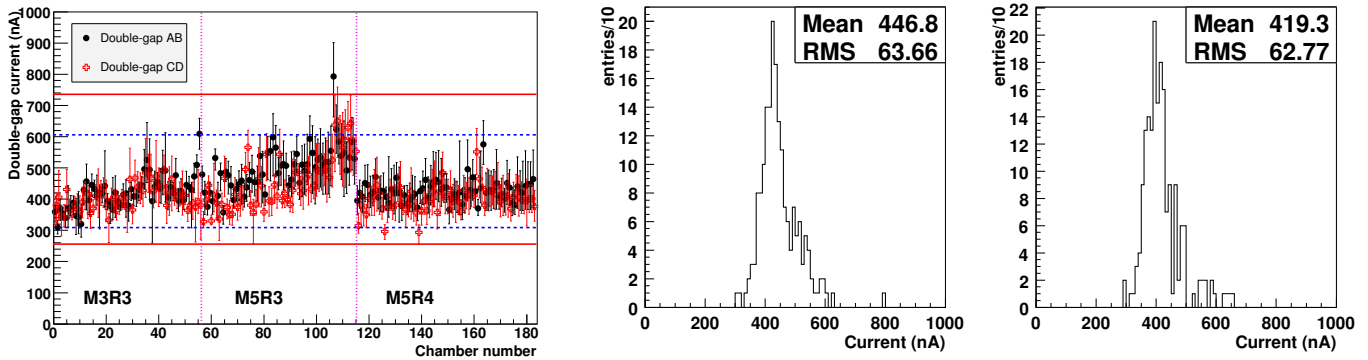


Figure 16  $\bar{I}_g^c$  values for all the gaps of the 184 chambers tested.

### 3.10 Gain equalization

All the source test were performed with the chamber supplied with an high voltage value of 2750 V. In figure 17 the values of all the  $\bar{I}_b^c$  are reported. Vertical bars indicate the maximum current spread of each double-gap. It is still possible to see that there is a number of chambers with region outside the limits of Categories I and II. Among those there are the chambers classified *spare* or *rejected*.

On the experiment it will be possible to tune the high voltage values in order to equalize the gain of the chambers. In particular we made the exercise to see what the situation would be like in the case all the double-gaps are operated at the same gain. In figure 18 the values of the total current spread found in each double-gap are reported once the mean gain values ( $\bar{I}_b^c$ ) of each double-gaps were equalized to 433 nA. In the case that the gain of all the double-gaps are equalized, all the chambers produced at LNF can be classified *good*.



**Figure 17** Values of  $\bar{I}_b^C$  for the double-gaps of all the 184 four-gap chambers tested. Vertical bars indicate the maximum current spread found.

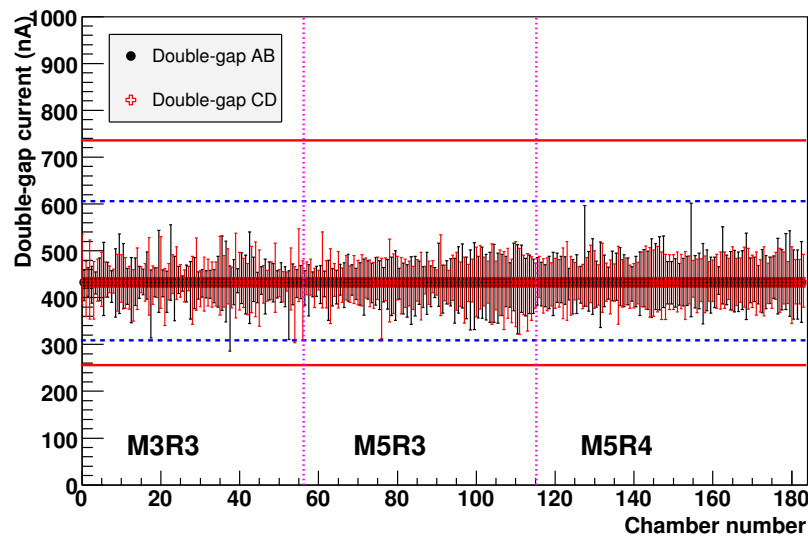


**Figure 18** Total gain spreads for the double-gaps of all the 184 four-gap chambers tested rescaled in order to equalize the values of  $\bar{I}_b^C$ .

## Conclusions

The results of the quality tests performed on 185 four-gap chambers produced at LNF have been presented. The wired panels used for the chamber production have undergone tests on the wire pitch and mechanical tension, whose results demonstrate the high quality achieved in the panel preparation. The gas tightness of the chambers was tested: only 6 chambers over the 185 built have a gas leakage larger than the experiment requirements and in five of them this problem will be probably fixed. The gain uniformity measurements performed on each chamber have been presented in detail. After correcting for the effect of the gas temperature and pressure variations, the gain uniformity of all the gaps and different chambers has been presented. Results showed that all the M3R3 chambers tested but one (number 58) can be classified *good* as well as 55 (out of the 59) produced M5R3 chambers and all the 68 M5R4 ones.

Moreover, if operated with different high voltage values in order to equalize the gain of all the double-gaps, all the 184 chambers tested can be classified *good*.



## Acknowledgments

The authors would like to thank all the production staff that made a superb job building the chambers and people who helped performing all the test. In particular the LNF team (M. Anelli, D. Carbinì, A. Di Virgilio, R. Rosellini and M. Santoni), the Russians (S. Smirnov, D. Belosludtsev, S. Kakourine and I. Fedotov) and especially V. Bocci for the precious private communications.

## References

- [1] LHCb Collaboration, "LHCb Muon System Technical Design Report", CERN/LHCC 2001-010 (2001) and "Addendum to the Muon System Technical Design Report", CERN/LHCC 2003-002 (2003).
- [2] M. Anelli *et al.*, "Quality tests of the LHCb muon chambers at the LNF production site ", IEEE Trans.Nucl.Sci.53:330-335,2006.
- [3] M. Anelli *et al.*, "Test of MWPC prototypes for Region 3 of Station 3 of the LHCb muon system", CERN-LHCB-2004-074.
- [4] A. Sarti, "A tool for the LHCb MWPC production monitoring: the LNF on-line database", CERN-LHCB-2006-037.
- [5] D. Pinci and A. Sarti, "Production and test of the LHCb Muon Chambers", presented at Hadron Collider Physics Symposium (HCP05), Les Diablerets, Switzerland July 4-9, 2005.
- [6] P. Ciambrone *et al.*, "Automated wire tension measurement system for LHCb muon chambers," Nucl. Instrum. Meth. A **545** (2005) 156.
- [7] MWPC Engineering Design Review, "Chamber requirements and specifications," W. Riegler, Available on-line: <http://indico.cern.ch/conferenceDisplay.py?confId=a03841>.
- [8] D. Pinci and A. Sarti, "Study of the MWPC gas gain behaviour as a function of the gas pressure and temperature," CERN-LHCB-2005-079.